

**A MATHEMATICAL AND EXPERIMENTAL INVESTIGATION OF
THE STACK COMPRESSION OF FILMS**

by

Albert W. Forrest, Jr.

DuPont Company
Circleville, Ohio

ABSTRACT

An analytical model has been developed which predicts the stack stiffness of multiple layers of films with rough surfaces. Film surfaces are approximated by asperity distributions measured using commercially available equipment. Comparisons were made with stack compression measurements made in a vacuum. It was found that measurements taken in a vacuum were quite different from those taken in air. Approximate correlations are included for PET films. The results are suitable for approximating the radial elastic modulus in rolls of film.

NOMENCLATURE

B	Asperity space and height distribution	M	Total number of asperities per unit area
b	Asperity width	m	Number of asperities larger than a defined value
C	Plate bending constant (see Equation 4)	N	Number of contacting asperities
d	Average gap between film layers	P	Pressure on film stack
D_r	Flexural rigidity of the film = $E_1 t^3/[12(1-u^2)]$	Q	Exponential distribution of asperity heights
E_1	Elastic modulus of film	R	Radius of curvature of asperities
E_2	Elastic modulus of the asperities	s	Spacing between contacting asperities
E'	Effective modulus (see Equation 3)	S_0	Radius of unit area
e	Compressive strain	t	Film thickness
F	Force on asperity pair (see Figure 1)	u	Poisson's ratio
G	Probability defined by Equation 11	W	Displacement at asperity contact
K_1	First stack compression coefficient	X	Asperity aspect ratio (see Figure 4)
K_2	Second stack compression coefficient	y	Bending displacement of film layer
		z	Asperity height

θ Asperity spacing distribution	ϕ Asperity height distribution function
σ_e Variance of the film surface roughness	Φ Asperity count in a set height range

INTRODUCTION

Understanding how film behaves in stacks or in multiple layers is key to the understanding of film winding and wound roll formation. Previous investigators [1-4] have shown that the stresses that form in wound rolls of film are key to the formation of different types of defects. Stress calculations depend on a knowledge of the winding parameters, the conditions on the surface of the winding roll and the properties of the film. Film properties for single sheets are routinely measured but the radial properties in a roll of film require knowledge of the properties of a stack of film. These properties are dependent on the single sheet properties and particularly the surface roughness. Pfeiffer and others [5-7] have measured the stack compression of films and found that they have either a hysteresis between the compression and decompression cycles or that they were compression rate dependent. All of these investigations have one thing in common. They measured the stack compression of the films in air.

The work presented here includes stack compression measurements in a vacuum. This was found to greatly reduce the hysteresis in the measured properties of the stack. A mathematical model also is included that uses the asperity distribution on the film surface along with the single sheet properties to predict the stack stiffness of the film. Greenwood [8,9] used this statistical approach to model the interaction of two surfaces. This work was limited to semi-infinite solids and it had to be extended to include a multi-layered stack of film where the layers can deflect near asperities.

Stack Compression and Film Winding

During the winding of film a number of things happen. The first stage occurs before the material begins to act as a composite. Here, any lack of flatness in the layers is removed and the film achieves a small but significant degree of contact. This happens at the surface of the winding roll and is usually assisted by the use of a layon roll. After initial contact is achieved, the compressive load is carried by asperity-to-substrate contact, film-layer bending, compressed air between the layers and possibly asperity-to-asperity contact.

The amount of air pressure between the layers is dependent on the winding conditions, the layon roll pressure and the associated geometries. It is not a fundamental property of the film stack. Measuring the film properties should not include, therefore, the effects of air between the layers. In the actual winding situation where inter-layer air does exist, accurate modeling can be achieved by using the ideal gas laws. Both the analysis and the stack compression experiments are conducted assuming the gaps between layers of film are evacuated. For the model this is accomplished by ignoring air pressure terms. For the experiments this is accomplished by measuring the stack compression in a vacuum.

ANALYTICAL MODEL FOR STACK COMPRESSION

The physical model used in the analysis is shown on Figure 1 where the simplest possible interaction is pictured. Here, we have a single layer of film supporting a compressive load through

two asperities. The procedure used is to develop a relationship between the compressive force and the displacement for an arbitrary asperity height and spacing. Then sum the effect of all of the asperity contacts that should occur using statistical surface data. If you think of the asperities as small springs (see Figure 2) you can see how the forces add and create the exponential stack compression curve that normally occurs.

There are several assumptions inherent in this approach. As discussed before, it includes no air between layers. It also ignores the statistically improbable asperity-to-asperity contact and contacts involving more than two asperities. The final assumption employed involves the method used to determine the spacing between the two asperities. Here, one asperity was considered and the probability of finding an asperity a distance s away in a given height range was determined. This interaction was then used in the accounting procedure to establish the relationship between the force and displacement. The assumption inherent to this is that only nearest neighbors interact. This should become more apparent as we develop the relationships.

Using the geometry shown in Figure 1, it is apparent that there are two types of deflection taking place as the load is transmitted. The asperity-to-surface interface undergoes a deflection w . The layer of film also deflected between the two asperities by an amount y . The sum of these two deflections due to some force F is the total deflection at that point. The first relationship we need is for the total deflection at that point which is

$$z - d = w + y \quad (1)$$

where all variables are defined in the nomenclature. Note that both the plate bending and the contacting asperities carry the same load F .

The asperity-to-substrate deformation is considered in the same way that Greenwood[8,9] approached the problem for the contact of rough solids. Here, the well known solution [10] for the contact of a sphere and a solid surface is employed and the result is

$$F = 1.333 E' R^{0.5} w^{1.5} \quad (2)$$

where E' is the effective elastic modulus given by

$$1/E' = (1-u_1^2)/E_1 + (1-u_2^2)/E_2 \quad (3)$$

and R is the radius of curvature of the contacting asperity.

The basic relationship for plate bending was obtained from Roark[11] and is

$$F = \frac{D_r Y}{C s^2} \quad (4)$$

where the constant C will be adjusted to produce the best fit with the actual stack compression data. If we equate the forces in Equations 2 and 4 and eliminate y by using Equation 1 we have the key relationship

$$1.333 C s^2 E' R^{0.5} w^{1.5} + D_r w + (d-z) D_r = 0 \quad (5)$$

which for a given set of asperity geometries and film gap can be used to calculate w which in turn is used in Equation 2 to calcu-

late the force for that interaction. The pressure at any given average film gap can be determined by summing all the forces for all the contacts over a given area. The equation for this is

$$P(d,..) = \sum_{i=1}^N F_i = \sum_{i=1}^N 1.333 E' R^{0.5} w^{1.5} \quad (6)$$

where N is the number of asperities contacting per unit area and all variables are adjusted to fit each asperity.

The summation in Equation 6 cannot reasonably be performed as written and a distribution function approach is required. A double distribution function is defined to accomplish this as

$$m(z,dz,s,ds) = M \int_z^{z+dz} \int_s^{s+ds} B(z,s) ds dz \quad (7)$$

where $m(z,dz,s,ds)$ is defined as the number of asperities with heights between z and $z + dz$ and with a first opposing asperity at a distance between s and $s + ds$. Note that only the first opposing asperity is considered and clusters involving more than two asperities are not included. Then Equation 6 can be rewritten as

$$P(d,..) = 1.333 M E' \int_d^\infty \int_0^\infty R^{0.5} w^{1.5} B(z,s) ds dz \quad (8)$$

which is a simple calculation once $B(z,s)$ and R are obtained.

The double distribution function is evaluated based on the assumption that the asperity height distribution is measured and that the asperities are randomly distributed over the film surface. With these assumptions

$$B(z,s) = \phi(z) \theta(s) \quad (9)$$

and $\phi(z)$ is obtained directly from measurements of the asperity distribution so that

$$\phi(z, z+dz) = M \int_z^{z+dz} \phi(q) dq \quad (10)$$

where $\phi(z, z+dz)$ is the number of asperities with a height between z and $z + dz$. This relationship can be evaluated directly from the measured asperity distributions.

Figure 3 shows a sketch of the geometry used to establish the second probability function required. Here, we need to consider the situation where one of our two asperities is contacting at the center of the circle. The circle radius S_0 is set to be a unit area over which N asperities are contacting. The number of asperities contacting is of course dependent on the average film gap and the asperity height distribution. The probability of one asperity contact between 0 and s is

$$G = 1 - (1 - s^2/S_0^2)^N \quad (11)$$

The probability of the first contact being between s and $s + ds$ is obtained from this basic relationship and is

$$G \Big|_s^{s+ds} = \left[1 - \left(1 - \frac{(s+ds)^2 - s^2}{S_0^2 - s^2} \right)^N \right] \left(1 - \frac{s^2}{S_0^2} \right)^N \quad (12)$$

and this is also a defining relationship for the other distribution function which is

$$N G \Big|_s^{s+ds} = N \int_s^{s+ds} \theta(g) dg \quad (13)$$

The final variable to be defined is the radius of curvature of the asperities. It has already been assumed that the contacting portion of the asperity is spherical. To define the radius of curvature at the contact point, we need to include the aspect ratio of the asperity as illustrated in Figure 4. Using this configuration the curvature becomes

$$R = z \left[\frac{x^2}{8} + \frac{1}{2} \right] \quad (14)$$

where X is the aspect ratio b/z.

To use the measured asperity height data, a numerical solution to Equation 8 must be employed. This also simplifies the evaluation of Equation 13, since over the incremental values of s the integral can be replaced by G, the probability function. The equation system used for the final calculations is

$$P(d,..) = 1.333 M E' \Sigma_{z=d}^{\infty} \phi(z, z+\delta z) R^{0.5} \Sigma_{s=0}^{\infty} w^{1.5} G \Big|_s^{s+ds} \quad (15)$$

with Equations 5, 10, 12, and 14 supplying needed relationship. The result of each evaluation is a pressure at a given average film gap d. This is then converted into strain and a pressure versus strain curve is generated.

STACK COMPRESSION MEASUREMENTS

The apparatus used to obtain the stack compression data is shown on Figure 5. This unit was designed to fit into an Instron testing machine and uses the load cells and operating speeds available on this device. The circular test plates have an area of 25.8 square centimeters (4 in²) and are enclosed in a volume that can be evacuated. A stack of film is produced by cutting the film using a circular die with a slightly larger diameter (6.35 cm) than the test plates. The vacuum ring is made of transparent plastic pipe so that the test can be viewed. An LVDT is included to establish the gap between the test plates.

Key film measurements are made in conjunction with the stack compression test. The film thickness is measured carefully using a mechanical dial gage with a ball-shaped foot having a 0.318 cm diameter. A second thickness measurement is calculated from measurements of the film density, the number of layers in the stack and the diameter of the test stack. The film surface topology is established using a Microscopical Image Analyzer (MIA). This is a device designed and built in DuPont for surface measurements. The roughness distribution is obtained by summing the asperity counts starting from the largest and plotting the results. This process is summarized for a 5 micron capacitor film on Figure 6.

The measured stack of film is inserted into the device as shown on Figure 5 and then placed in an Instron testing machine. The test volume is evacuated to approximately 725 mm of Hg. Prior to compressing the film, the load cell is zeroed to account for the force produced by the vacuum. At least one compression and decompression cycle is obtained for each film tested. A compression

and decompression head speed of 0.5 mm/min is used. Some preliminary tests were conducted in air to establish the effect of vacuum testing.

COMPARISON OF RESULTS

The most complete set of data is presented for the 5 micron capacitor film discussed previously (see Figure 6 And Table 1). Figure 7 shows a plot of the experimentally obtained stack compression cycle obtained with and without a vacuum. Notice the dramatic difference between the in-air and in-vacuum results. The air adds a false effect that appears to be hysteresis or a rate effect. All of the films tested in air exhibited this same characteristic and only test results measured in a vacuum will be presented from this point on.

A comparison between the analytical and experimental results is shown on Figure 8. This again is the 5 micron capacitor film with the surface data shown on Figure 6. A film bending constant of 0.25 was obtained empirically and is used for all of the analytical results. The film thickness was the average of the micrometer and weight measurements. All other film properties and measurements are shown on Table 1.

A quantitative comparison is made by obtaining the stack compression coefficient, K_2 , for all the films tested. This coefficient appears in Pfieffer's [5] work in an exponential curve fit of his stack compression results. Here, K_2 is an exponential slope factor defined by

$$P = K_1 \exp(K_2 e) - K_1 \quad (16)$$

and is a good factor to compare the stiffness of different film stacks. For the 5 micron capacitor film, K_2 from the measured data is 54 and 58 for the compression and decompression, respectively. The analytical results yield a K_2 of 57 which is between the two measured values and less than 6% from the compression data. The agreement for this particular film is excellent but to fully test the analytical procedure we need to look at a number of films.

Three additional test films are included ranging from 2 to 36 microns in thickness with both smooth and relatively rough surfaces. The results for these tests are shown on Tables 1 and 2 and Figures 9 through 14. The measured film property data is included as Table 1. The surface measurements are included on Figures 9, 11 and 13 for the 2, 14.5 and 36 micron films, respectively. The even numbered plots show both the measured and calculated stack compression results. Table 2 has the K_2 results for both the measured and calculated stack compressions.

Film thickness also was adjusted to account for surface roughness and to improve the fit with the experimental data for all the films except the 5 micron capacitor film. This was necessary because we had difficulty in determining the initial zero stress and strain point and there is an effect that occurs on the first compression that the model does not consider adequately. Both of these points will be discussed in more detail later.

The agreement for the stack stiffness coefficient is good with the exception of the compression cycle of the 36 micron film where the difference is 36%. Several compression and decompression cycles were run for the 36 micron film to try and better understand this disagreement. The plotted results for this is presented on Figure 15. This plot shows that some cycle dependent deformation does occur between the first and third test cycle. Note that the third cycle compression and decompression have very nearly collapsed to the first stage decompression cycle. Here, the measured and calculated values for K_2 differ by only 12%.

SIMPLIFIED RELATIONSHIP FOR PET FILM

The analysis as described is complicated and general enough to describe the response of a wide variety of films. All of the data collected thus far is for PET films, however, and a simple correlation would be preferred. To accomplish this, the first step is to characterize the film surface in a more compact way. This can be done by using an exponential distribution function described by

$$Q(z) = \frac{1}{\sigma_e} \exp\left(-\frac{z}{\sigma_e}\right) \quad (17)$$

The reciprocal of the variance of the distribution, $1/\sigma_e$, is a measure of the slope of the asperity distribution (a smaller σ_e means a steeper slope). The number of asperities greater than or equal to z can be determined by

$$Q \Big|_z^\infty = M \exp\left(-\frac{z}{\sigma_e}\right) \quad (18)$$

where M is the total count of asperities.

The measured surface characteristics of the four cases considered previously are included on Table 2 in a form suggested by Equation 18. A simplified relationship was obtained for K_2 using this means to characterize the surface. For PET films it is

$$K_2 = 5.76 \frac{t^{0.54}}{\sigma_e^{0.96}} \quad (19)$$

where both t and σ_e are in microns. A plot of this correlation and measured stack compression data is shown on Figure 16. Note that data from additional films has been added to support the correlation over a wider range.

CONCLUSIONS

Stack compression measurements must be taken in a vacuum. Measurements in air include the effect of air flowing out from between the layers of film. This masks the effect of surface topology and film parameters. Calculations requiring information on the behavior of stacks of film should use the vacuum results for the film and model the air between layers using the ideal gas formulas.

The analytical procedure presented here predicts the stack stiffness reasonably well. Discrepancies between the measured and predicted values of K_2 are between 2% and 17% when the initial compression is not used.

Films typically have some differences between the first compression and subsequent decompressions and compressions. This may be plastic deformation or it may be an initial conformation between layers that does not fully repeat. Rolls of film that collapse radially after winding typically have gross defects that make them rejects. This type of ageing could be due to either escaping air or this first compression effect. Layon rolls are used to produce wound rolls that do not deteriorate with time. This may be due in part to the fact that the layon roll makes that initial compression of the film so that it does not creep after the roll is wound.

The relative uncertainty of the various film measurements and the difficulty in locating the zero strain point makes complete evaluation of the analytical model difficult. The fine

tuning process used to achieve the analytical stack compression results involved adjusting the plate bending factor C for the 5 micron capacitor film and holding it constant thereafter. The film thickness for other films also was adjusted slightly (see Table 1) so that the measured and predicted results matched at the end of the compression. This has the effect of shifting the predicted stress-strain curves in the strain direction without significantly effecting the slope (K_2).

A much simpler correlation is adequate for predicting the stack stiffness coefficient K_2 for PET films. It shows that the stiffness is proportional to thickness to the 0.54 power and the steepness of the asperity distribution to the 0.96 power. For a given film type and thickness, the sharpness of the asperity distribution is the primary factor controlling the relative stiffness of films. The total asperity count does not appear in the correlations developed directly but the additive concentration typically effects the slope of the asperity distribution.

More work needs to be done to check the analytical procedure presented here for other films and to modify it as necessary. All of the data presented here is for PET films. Other films may behave differently enough to make the assumptions used in this investigation invalid. The surface roughness data is measured using the Microscopical Image Analyzer. This unit is not widely available. The analysis and correlations should be repeated using other commercially available devices for surface measurement. An improved method of locating the zero strain point in the measured results and accurately measuring key film parameters must be developed before the analytical model can be completely evaluated.

Table 1 Film physical properties and measurements

Elastic modulus of film	3.79X10 ⁶ kPa
Elastic modulus of asoerities	68.9X10 ⁶ kPa
Poisson's ratio of film	0.4
Poisson's ratio of asperities	0.4
Aspect ratio of asperities	5.0

FILM THICKNESS(microns)

Type & nominal thickness	Measured by		used in
	micrometer	weight	calculation
Capacitor 5 micron	4.85	5.05	4.95
Capacitor 2 micron	1.85	2.06	2.08
Video 14.5 micron	14.1	14.1	14.1
Graphic 36 micron	35.2	35.8	34.5

Table 2 Stack compression results

Film type	5C	2C	14.5VB	36G
Asperity count/sqmm	15200	28000	8100	7500
Surface variance S_e	0.212	0.192	0.192	0.267
K_2 Experimental comp	54	41	128	108
K_2 Experimental relax	58	54	131	131
K_2 Solution	57	48	125	147
K_2 Correlation	61	42	117	138

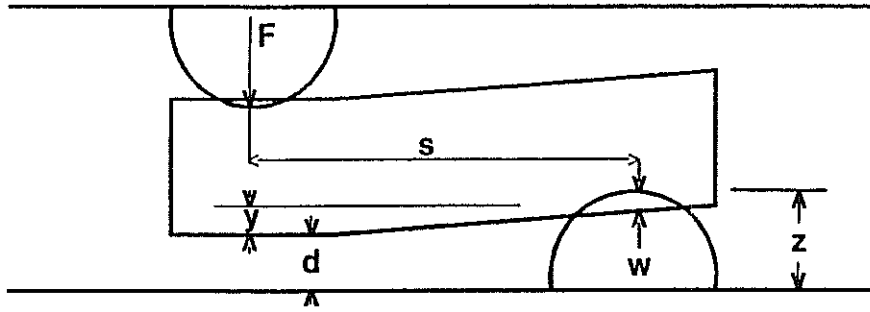


Fig. 1 Two-asperity model for stack compression of film

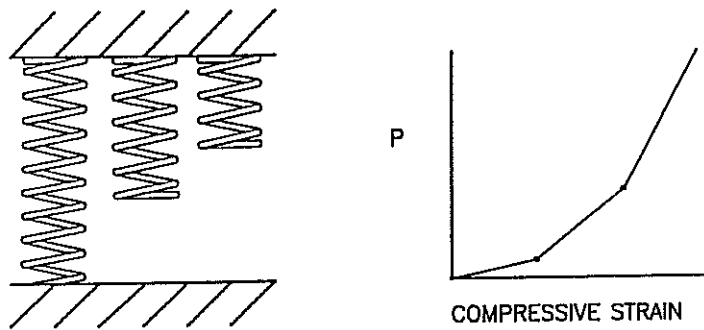


Fig. 2 Spring analogue for stack compression

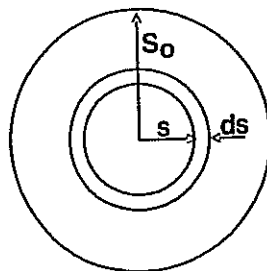


Fig. 3 Geometry for spacing distribution function

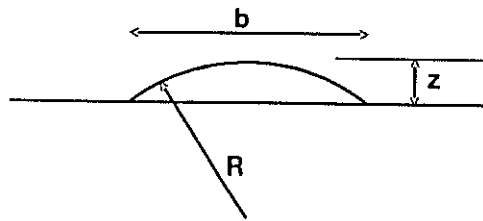


Fig. 4 Definition of the aspect ratio factor

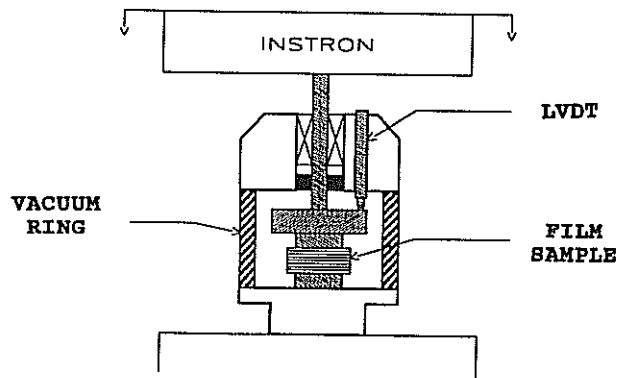


Fig. 5 Vacuum stack compression test fixture

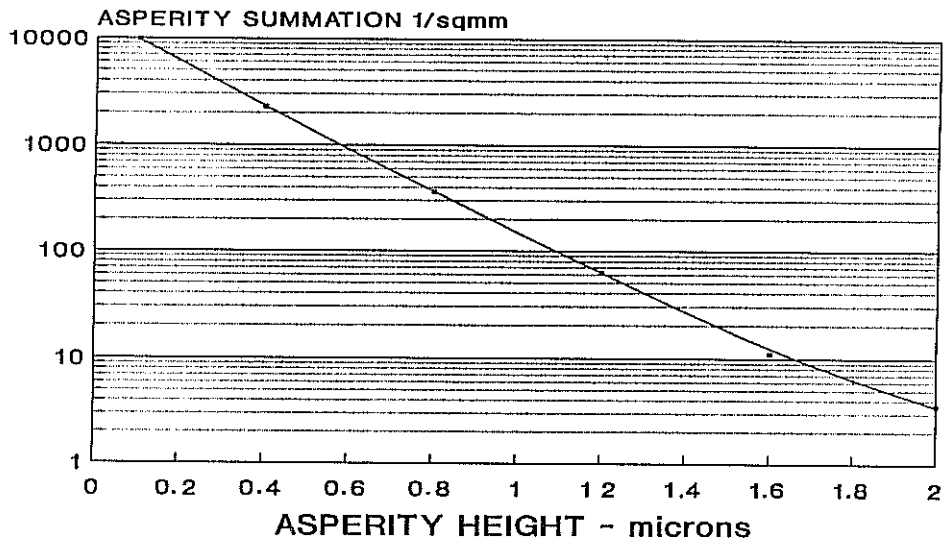


Fig. 6 Asperity distribution for the 5 micron capacitor film

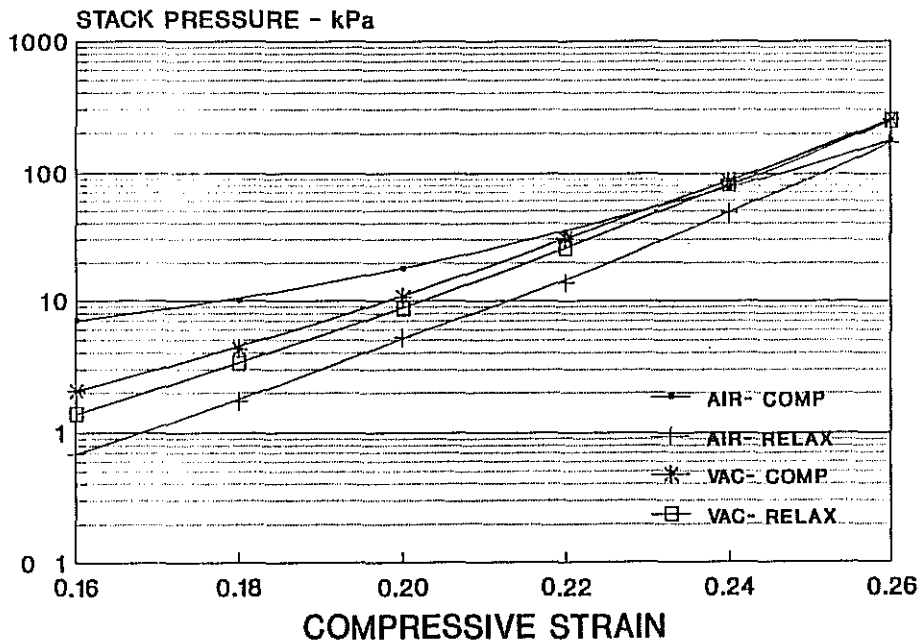


Fig. 7 Stack compression measurement results in air and in a vacuum

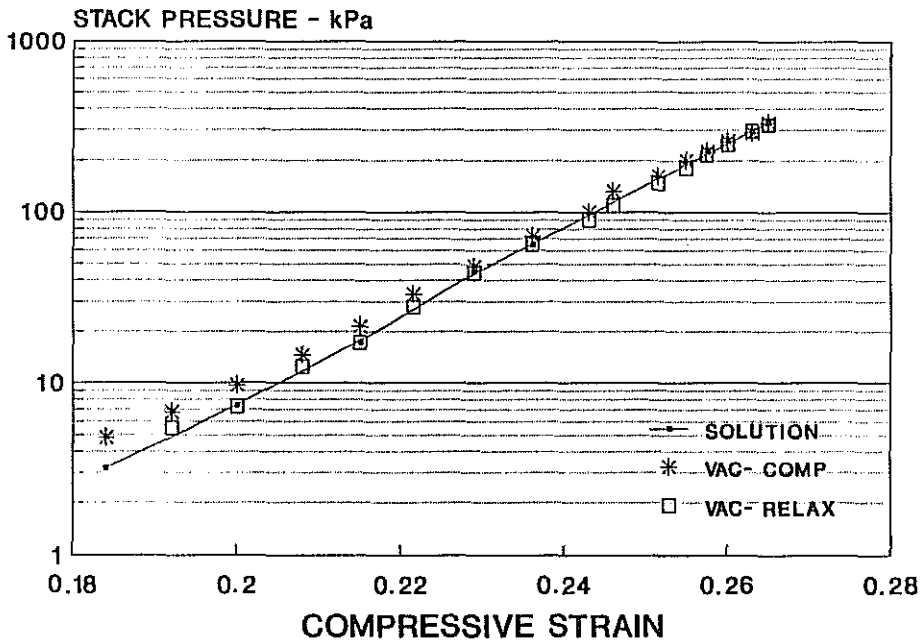


Fig. 8 Comparison between the analytical and experimental stack compression results for 5 micron capacitor film

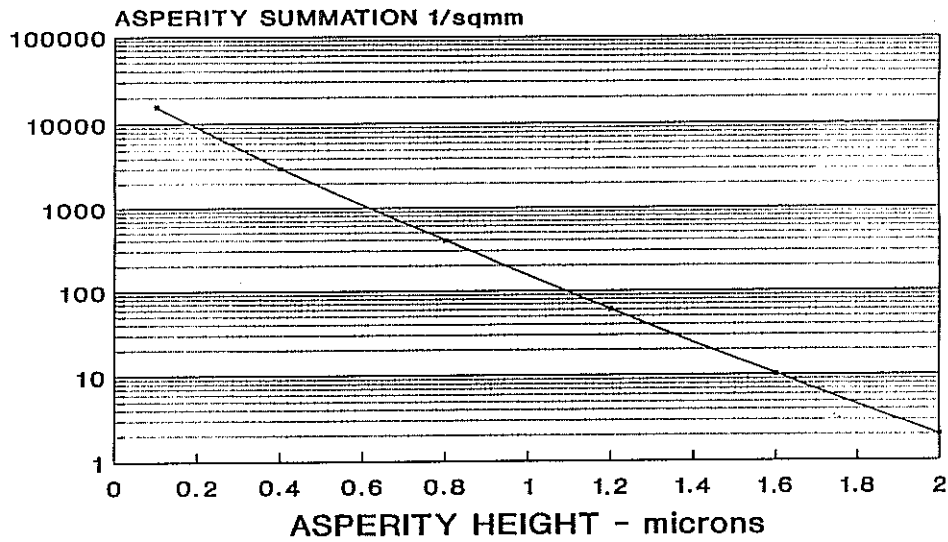


Fig. 9 Asperity distribution data for 2 micron capacitor film

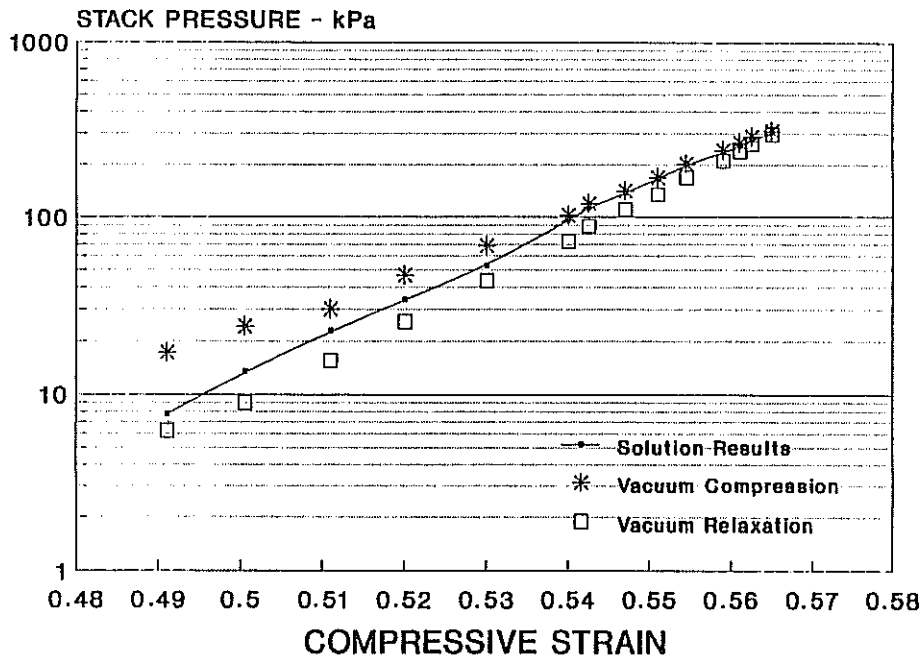


Fig. 10 Comparison between the analytical and experimental stack compression results for 2 micron capacitor film

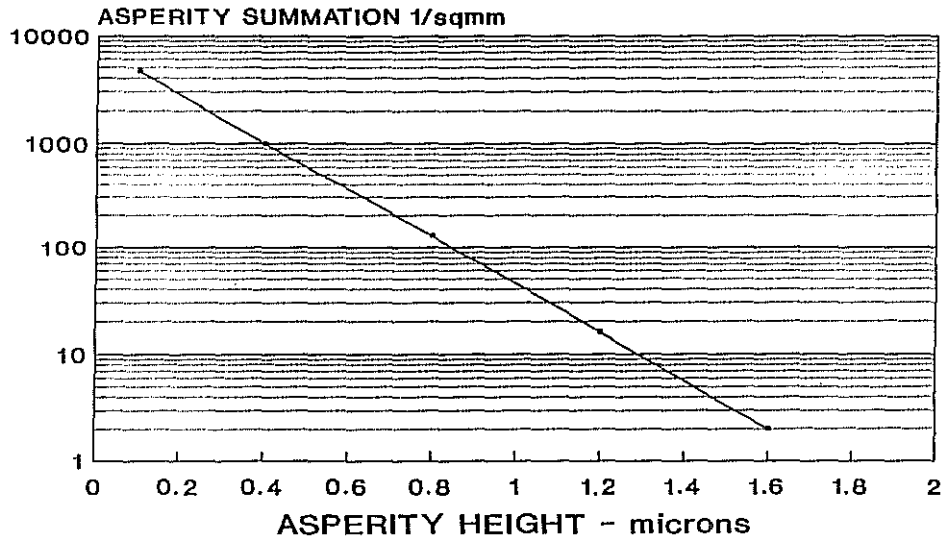


Fig. 11 Asperity distribution data for 14.5 micron video film

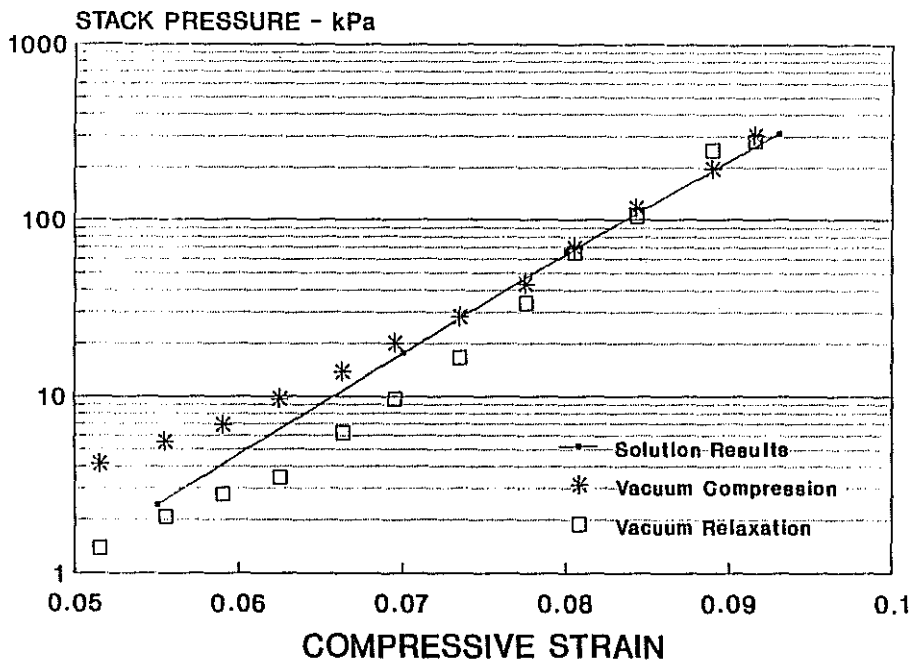


Fig. 12 Comparison between the analytical and experimental stack compression results for 14.5 micron video film

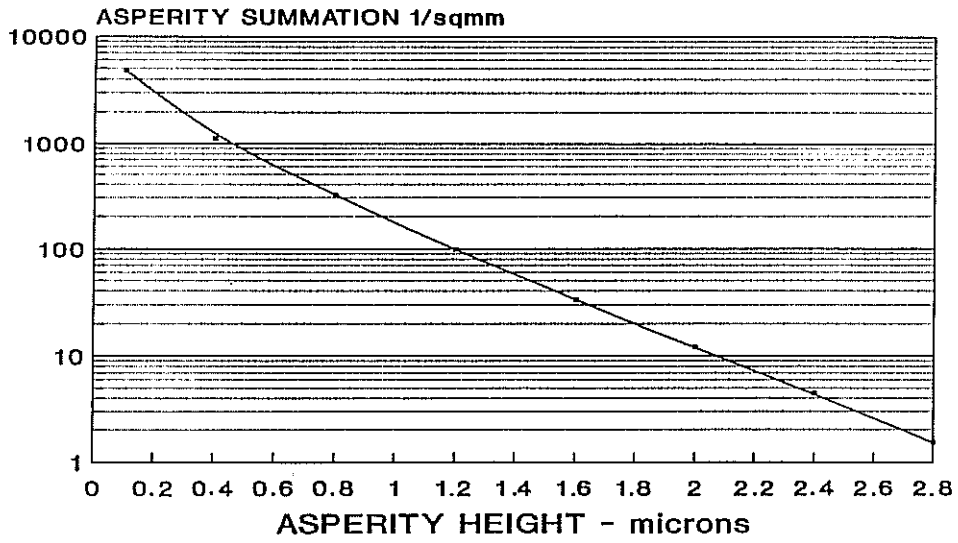


Fig. 13 Asperity distribution data for 36 micron graphics film

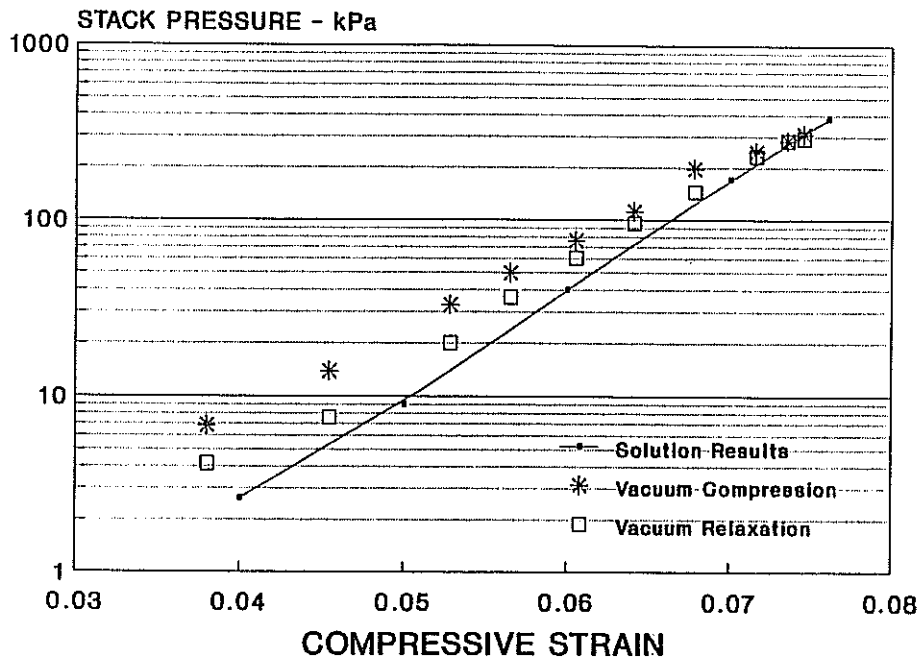


Fig. 14 Comparison between the analytical and experimental stack compression results for 36 micron graphics film

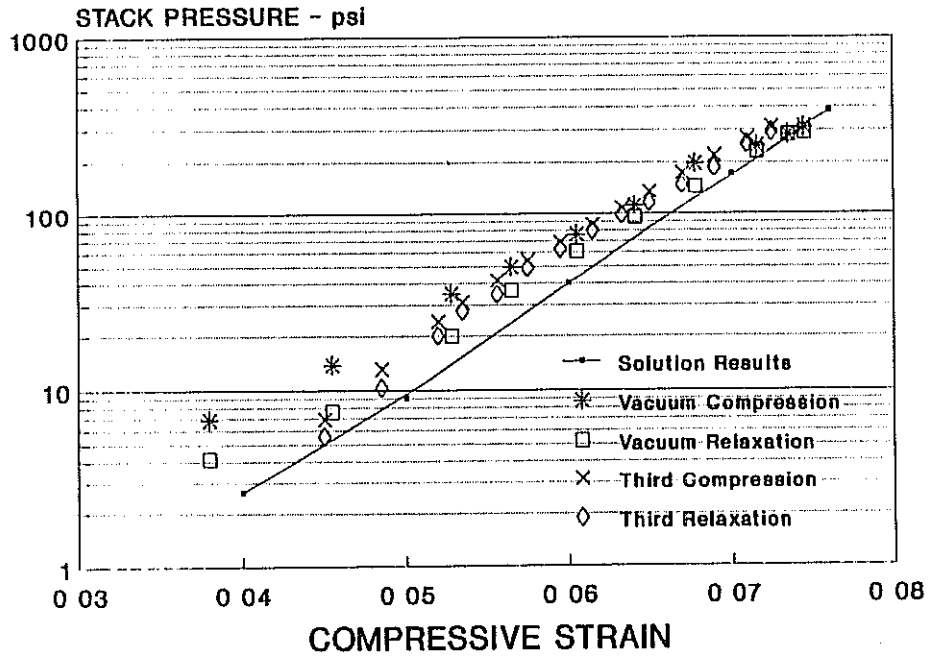


Fig. 15 Stack compression results for multiple cycles of 36 micron graphics film

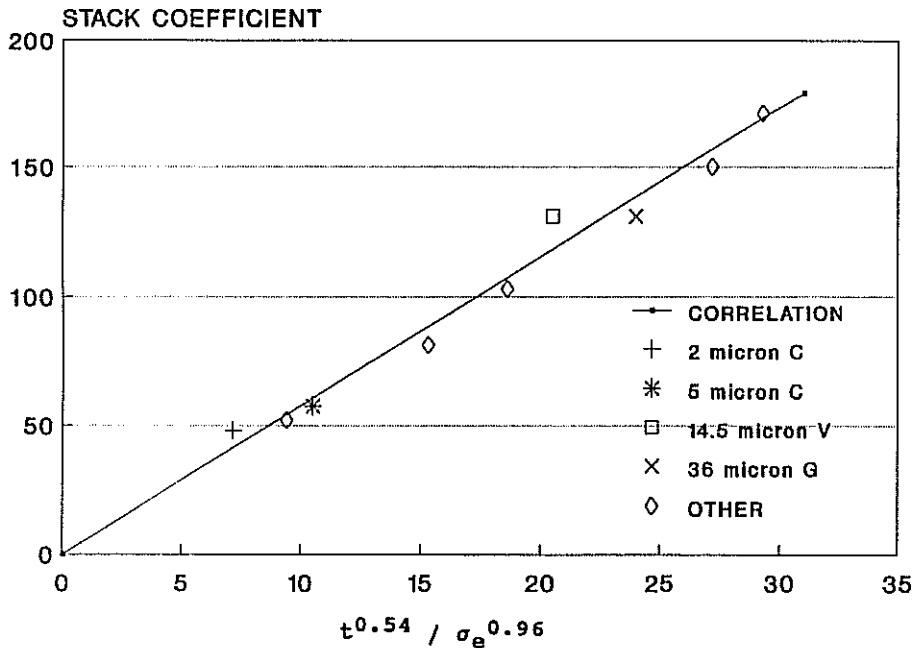


Fig. 16 Simplified K_2 correlation for PET films

BIBLIOGRAPHIC REFERENCES

1. Pfeiffer, J. D., "Internal Pressures in a Wound Roll of Paper", Tappi, Vol 49, No. 8, pp. 342-7, August 1966.
2. Pfeiffer, J. D., "Prediction of Roll Defects from the Structure Formulas", Tappi, Vol 62, No. 10, pp. 83-85, 1979.
3. Lee, Bang-Eop, "Buckling Analysis of Starred Roll Defects in Center Wound Rolls", Ph.D. Thesis at Oklahoma State University, May 1991.
4. Struik, L. C., "Film Winding Project", Quarterly Reports 1, 2 and 3, Netherlands Organization for Applied Research (TNO) Reports No. MRPIII-78/2 and MRPIII-78/4, 1978.
5. Pfeiffer, J. D., "Measurements of the K_2 Factor for Paper", Tappi, Vol 64, No. 10, pp. 130-1, 1981.
6. Good, J. K.; Brewster, Gayla and Price, Laura, "Measurement and Characterization of the Constitutive Properties of Web Stacks", ongoing Project at Oklahoma State University, WHRC Project Report, October 1991.
7. Good, J. K. and Qualls, W. R., "Theoretical and Experimental Studies of Viscoelastic and Hygroscopic Effects in Wound Rolls", ongoing Project at Oklahoma State University, WHRC Project Report, October 1991.
8. Greenwood, J. A., "The Area of Contact Between Rough Surfaces and Flat", Journal of Lubrication Technology, ASME Transactions, pp. 82-91. January, 1967.
9. Greenwood, J. A. and Tripp, J. H., "The Contact of Two Nominally Flat Rough Surfaces", Proceedings of the Institute of Mechanical Engineers (185), pp. 625-33, 1970-71.
10. Timoshenko, S. and Goodier, J. N., Theory of Elasticity, McGraw-Hill Book Company, 1951.
11. Roark, R. J., Formulas for Stress and Strain, McGraw-Hill Book Company, Fourth Edition, p. 218, 1965.

QUESTIONS AND ANSWERS

- Q. How do you obtain the variance of the film surface roughness?
- A. Basically, it's a measurement. We used a microscopical image analyzer. It metallizes the film at a very acute angle, coming down close to the surface, and then, there's a shadow formed by the metallization on the back side of the asperity and you measure the shadow and infer the heights from the shadow. It's an internal piece of equipment developed at DuPont.
- Q. What's the relationship between S (the spacing between contacting asperities) and the film thickness?
- A. S to the thickness of the film? It really ranges, because S can be any number. It's just in a distribution – part of a probability type thing. It can go from 0 on up, but the probability of having an appreciable number of (first contact) asperities at a large S becomes extremely small when you have a substantial number of asperities contacting.
- Q. There are better mathematical relationships describing the contact between a sphere and a surface. Why didn't you use these relationships?
- A. I'm sure that a higher degree of sophistication could be put into either the plate bending or the Hertzian type of contact. Again, the idea was to come up with

the simplest thing because you're going to have to do this in such a repetitive fashion in the analysis to figure out the stress versus the strain.

Q. How did you develop the correlation for K_2 ?

A. It wasn't totally mathematical. A lot of it was just fitting experiments. We had observed, even from our stack compression in air, that K_2 seemed to be proportional to the half power of the film thickness, so we had a good start. Basically, I started around that and worked it out.

Q. Do you think that the type of additive used to create the film roughness can have an effect of the film surface? The complexity around modeling the asperity properties seems substantial.

A. Yes, there's so much, we use a number of different types of particulates in our films. The particulates are hard in comparison to the film. The asperities are actually polyester film covered particulates, as I'm sure you're well aware. Coming up with an exact value for the elastic modulus of asperities would be a study in itself.